

Upward and downward injection of Rossby wave activity across the
tropopause:
A new aspect of the troposphere-stratosphere dynamical linkage

By Kazuaki NISHII and Hisashi NAKAMURA * †
University of Tokyo, Japan

(Submitted in June 2003, Revised in July 2004)

SUMMARY

Propagation of zonally-confined Rossby wave activity between the troposphere and lower stratosphere of the southern hemisphere during austral winter and spring of 1997 is studied, by using a wave-activity flux and refractive index both defined for stationary Rossby waves on a zonally-asymmetric time-mean flow. A particular event of large-scale, quasi-stationary cyclogenesis in the troposphere is discussed, to which downward wave-activity injection from anticyclonic anomalies upstream that had developed in the exit region of the lower-stratospheric polar-night jet (PNJ) contributed substantially. Consistent with that downward injection, phase lines of observed streamfunction anomalies exhibited a distinct eastward tilt with height. The development of the anticyclonic anomalies occurred at the leading edge of a quasi-stationary Rossby wave train propagating along the PNJ that had originated from a tropospheric blocking ridge farther upstream. Though less often than upward wave-activity injection across the tropopause, similar events of downward wave-activity injection occurred several times during that season, primarily in the regions south of Australia and over the central South Pacific, over each of which the PNJ exit overlapped with a tropospheric subpolar jet to form a vertical waveguide locally. It is argued that the downward wave-activity propagation is essentially due to refraction in the vertically sheared westerlies, and the zonal asymmetries in the time-mean flow are a likely factor for the observed geographical preference of the downward wave-activity injection.

KEYWORDS: Blocking Cyclogenesis Low-frequency variability Polar-night jet Refractive index Wave-activity flux

1. INTRODUCTION

The planetary-scale dynamical linkage between the stratosphere and troposphere has been discussed with respect mainly to the upward influence of the tropospheric processes, in recognition of the fact that the source of upward

* Additional affiliation: Frontier Research Center for Global Change, Yokohama, Japan

† Corresponding author: Hisashi Nakamura, Department of Earth and Planetary Science, Graduate School of Science, University of Tokyo, Tokyo, 113-0033 Japan. E-mail: hisashi@eps.s.u-tokyo.ac.jp

propagating planetary waves is in the troposphere. For example, a stratospheric sudden warming (SSW), which is one of the prominent features in the wintertime stratosphere, is characterized by the marked deceleration of a westerly polar-night jet (PNJ), in association with the breakdown of the non-acceleration condition for planetary waves propagating upward from the troposphere (e.g., Matsuno 1971). More generally, modulations of the stratospheric zonal-mean westerlies are caused by their interaction with upward propagating planetary waves (e.g., Hirota and Sato 1969; Shiotani and Hirota 1985).

Some studies, however, have examined the *downward* dynamical influence from the stratosphere to the troposphere. For example, Geller and Alpert (1980) argued on the basis of their numerical experiment that variations in the stratospheric PNJ induced by the anomalous solar ultraviolet radiation could influence the tropospheric circulation by modifying vertically propagating planetary waves. Likewise, Boville (1984) showed through his model experiments that changes in the stratospheric PNJ could alter the tropospheric circulation characteristics by modulating planetary wave propagation. Kodera *et al.* (1990) found that the enhanced upper-stratospheric PNJ in December tends to be followed by the stronger westerlies over the tropospheric polar region in February. In that process, weak anomalies in the zonal-mean zonal wind first appear in the stratosphere and then propagate downward into the troposphere within a month, accompanied by anomalous meridional propagation of planetary waves (Kodera *et al.* 1991). Kodera and Chiba (1995) argued that during and after an SSW event, the modification in the zonal wavenumber 2 ($k=2$) component of tropospheric planetary waves tends to give rise to a surface cold surge, which leads to the enhancement

of stormtrack activity in the North Atlantic and the subsequent blocking formation downstream. Yoden *et al.* (1999) showed through a numerical experiment that zonally-symmetric warm anomalies in the stratospheric polar region and the associated weak westerlies in midlatitudes both tend to propagate downward into the troposphere only during an SSW event in which the $k=2$ planetary-wave component plays a primary role. Through the potential-vorticity (PV) inversion technique, Hartley *et al.* (1996) showed that the anomalous polar vortex in the lower stratosphere can exert a significant influence upon the tropospheric circulation particularly over the North Atlantic. Essentially the same downward influence of the anomalous stratospheric polar vortex in the northern hemisphere (NH) on the troposphere as mentioned above has recently been discussed in the context of the Arctic Oscillation (AO) or the NH annular mode (NAM). In the cold season, AO anomalies that emerge rather irregularly in the stratosphere tend to propagate slowly downward into the troposphere within a few weeks (Baldwin and Dunkerton 1999; Kodera and Kuroda 2000ab; Kodera *et al.* 2000; Kuroda and Kodera 1999, 2001; Christiansen 2001; Thompson and Wallace 2001; Polvani and Kushner 2002; Zhou *et al.* 2002), which is considered to be associated with the interaction between the anomalous polar vortex and the anomalous propagation of planetary waves. Perlwitz and Harnik (2003; hereafter referred to as PH03) discussed the influence on the tropospheric circulation of the downward propagating planetary waves from the stratosphere that have originated in the troposphere and then been reflected back at a critical level in the stratosphere.

Most of the previous studies as mentioned above focused on the entire field of stratospheric planetary waves or their zonal harmonics in relation to the variability of a zonally-symmetric polar vortex and/or PNJ. However, not

much attention has been paid to localized circulation anomalies associated, for example, with zonally-confined Rossby wave trains. Specifically, not many attempts have been made to identify which particular localized circulation anomalies in the troposphere are the origin of given anomalous behavior of the stratospheric planetary waves. Randell (1988) was the first to present a statistical signature of Rossby wave trains in the wintertime stratosphere propagating upward from localized tropospheric origins in the southern hemisphere (SH). More recently, Nakamura and Honda (2002; hereafter referred to as NH02) showed that tropospheric circulation anomalies in February over the North Atlantic emit a quasi-stationary Rossby wave train upward into the lower-stratospheric PNJ over the Eurasian continent. Nishii and Nakamura (2004b) found that the breakdown of the SH polar vortex in late September 2002 that led to the collapse of the ozone hole was contributed to by a Rossby wave train propagating upward from a blocking flow configuration over the South Atlantic. Nishii and Nakamura (2004a; hereafter referred to as NN04) analyzed dynamical characteristics of submonthly geopotential height fluctuations observed in the SH lower stratosphere during late winter and early spring of 1997. They showed that those fluctuations were often associated with zonally-confined Rossby wave trains that had originated from quasi-stationary tropospheric anomalies. The upward and eastward propagation of those wave trains was found sensitive to the zonally-asymmetric PNJ structure, which can be regarded as an important factor for the zonally-asymmetric distribution of the activity of the submonthly fluctuations observed in the SH lower stratosphere.

Reviewing NN04's analysis, one may wonder what will happen for a zonally confined wave train as it keeps propagating through the lower-stratospheric PNJ.

One can image that a PNJ with a substantial westerly vertical shear, even if it were zonally uniform, would act as a “prism” that allows only the zonal wavenumber 1 ($k=1$) component (or maybe also the $k=2$ component) included in the wave train to transmit farther upward. The rest of the wave activity, associated mainly with the higher harmonics ($k \geq 2$), would be refracted back into the troposphere.

Figure 1 illustrates this “prism effect” of an idealized PNJ in a β channel by using the ray tracing method. The westerlies are zonally symmetric with a uniform vertical shear and Brunt-Väisälä frequency in the stratosphere (above the 10-km altitude). In contrast to PH03, in which downward propagation of Rossby wave activity was due to reflection of upward propagating planetary waves at a critical level, downward wave-activity propagation illustrated in Fig. 1 is due to *refraction* of wave activity in the vertically sheared westerlies. Furthermore, unlike in PH03, where the downward reflection of the entire planetary waves is discussed, our primary focus is placed on a zonally confined wave packet that accompanies geographically localized circulation anomalies. The anomalies are only a fraction of the entire planetary waves that are modulated due to the superposition of those anomalies on the climatological wave field.

In such an idealized situation as depicted in Fig. 1, the upward as well as downward injection of Rossby wave activity across the troposphere can occur at any longitude. In reality, however, the upward injection exhibits an apparent geographical preference even in the SH in the presence of zonal asymmetries in the seasonal-mean westerlies (NN04). One would find a similar geographical preference also for the downward wave-activity injection, if it really occurs, across the tropopause.

In this study, as an extension of NN04, we show several pieces of evidence that wave activity associated with zonally-confined Rossby wave trains in the SH lower stratosphere can indeed propagate *downward*, contributing positively to the development of localized circulation anomalies in the troposphere. The essential features of the downward wave-activity propagation observed in the SH are illustrated in a schematic diagram in Fig. 2. (i) Tropospheric circulation anomalies amplify at a particular location associated with an incoming quasi-stationary Rossby wave train and/or the local feedback forcing from synoptic-scale migratory eddies; (ii) wave activity emanating upward from the developed anomalies reaches the lower stratosphere, if exists, through a localized vertical waveguide or “chimney”, leading to the development of circulation anomalies with the opposite sign in the stratosphere; (iii) if a waveguide extends downstream along the PNJ, the wave activity propagates eastward along it, forming a zonally and meridionally-confined wave train in the lower stratosphere; (iv) anomalies developing at the leading edge of the lower-stratospheric wave train, if they reach the PNJ exit where another “chimney” forms, release part of the associated wave activity downward across the tropopause, contributing to the local development of tropospheric circulation anomalies with the opposite sign; and (v) downstream wave-activity emanation from the matured tropospheric anomalies occurs with the subsequent formation of another wave train in the troposphere, or in some occasions, wave activity re-emanates back into the stratosphere.

Localized in the zonal direction, the upward/downward wave-activity propagation associated with zonally-confined wavetrains cannot be well depicted in the conventional framework of the zonal harmonic decomposition nor the Eliassen-Palm (E-P) diagnosis. We will therefore adopt the same framework as in NH02

and NN04, in which the entire field at a given instance was decomposed into the three-dimensional, zonally-asymmetric time-mean flow‡ and deviations from it (*i.e.*, anomalies). Following those two studies, we applied diagnostics suited for that framework, in order to depict three-dimensional group-velocity propagation of quasi-stationary Rossby wave trains both in the troposphere and lower stratosphere.

2. DATA AND DIAGNOSTIC METHODS

As in NH02 and NN04, we use a reanalysis data set of the U.S. National Centers for Environmental Prediction (NCEP) and the U.S. National Center for Atmospheric Research (NCAR) (Kalnary *et al.* 1996). The data have been provided on a regular $2.5^\circ \times 2.5^\circ$ latitude-longitude grid at each of the 17 standard pressure levels from 1000 hPa up to 10 hPa. A low-pass digital filter with a cut-off period of 8 days has been imposed on the twice-daily data time series to remove high-frequency fluctuations associated with migratory, synoptic-scale disturbances. Seasonal evolution of the circulation is represented in the 31-day running-mean field, and the deviation of the low-pass-filtered field from the running-mean field corresponds to submonthly, quasi-stationary anomalies. Geopotential height anomalies have been multiplied by a factor (f_0/f) to mimic streamfunction-like anomalies (f : the Coriolis parameter; $f_0 = f(43^\circ S)$).

A wave-activity flux, formulated by Takaya and Nakamura (2001; hereafter referred to as TN01), is used for representing three-dimensional propagation of quasi-stationary Rossby waves in the zonally-inhomogeneous westerlies. Its

‡ In this paper, we use the term “time-mean flow” to indicate seasonally varying flow whose time scales are much longer than those of the evolution of quasi-stationary circulation anomalies.

expression in the logarithm pressure coordinate may be given as

$$\mathbf{W} = \frac{p}{2|\mathbf{U}|} \begin{pmatrix} U(v'^2 - \psi'v'_x) + V(-u'v' + \psi'u'_x) \\ U(-u'v' + \psi'u'_x) + V(u'^2 + \psi'u'_y) \\ \frac{f_0 R_a}{N^2 H_0} \{U(v'T' - \psi'T'_x) + V(-u'T' - \psi'T'_y)\} \end{pmatrix}, \quad (1)$$

where ψ' denotes perturbation geostrophic streamfunction, T' perturbation temperature, (u', v') perturbation geostrophic velocity, (U, V) the geostrophic basic-flow velocity, R_a the gas constant of dry air, H_0 the constant scale height, p the normalized pressure and N the Brunt-Väisälä frequency defined for the basic flow. In this study, the 31-day running-mean field is regarded as the basic state in which quasi-stationary waves are embedded, and the low-pass-filtered anomalies are regarded as fluctuations associated with those waves. This flux is suited for representing a “snapshot” of a propagating Rossby wave packet, because the flux is independent of wave phase and parallel to the local three-dimensional group-velocity vector or, more precisely, the “wave-activity velocity” (Harnik 2002). It is noteworthy that \mathbf{W} applied to quasi-stationary anomalies embedded in a zonally-varying time-mean flow accounts only for a fraction of the corresponding flux associated with the entire field of planetary waves that can be evaluated by using Plumb’s (1985) wave-activity flux. Thus, the vertical propagation of stationary Rossby wave trains can be either upward or downward depending on time and location, as exemplified in the following sections, despite the general tendency that the wave-activity flux of the entire planetary waves is upward because they are forced in the troposphere.

In addition, a refractive index (κ_s) is used for representing mean-flow properties with respect to the propagation of stationary Rossby waves. Following NH02 and NN04, we extend a particular index defined originally on a meridional

plane by Karoly and Hoskins (1982) into a zonally-asymmetric basic flow, in a manner similar to those in Karoly (1983) and Hoskins and Ambrizzi (1993):

$$\kappa_s^2 = \frac{|\nabla_H Q|}{|U|} - \frac{f^2}{4N^2 H_0^2}.$$

In this definition, ∇_H denotes a horizontal gradient operator, and Q , which signifies quasi-geostrophic PV of the basic flow, and all other quantities have been evaluated on the basis of the 31-day running-mean field as in NN04. To keep consistency with WKB-type assumptions used in the derivation of the wave-activity flux of TN01, we use locally evaluated N . As in Chen and Robinson (1992), the terms that include vertical derivatives of N , which were included in the definition by Karoly and Hoskins (1982), have been neglected in our evaluation of κ_s , in recognition of the fact that vertical variations in N are generally small except in the immediate vicinity of the tropopause. Still, a discontinuity is present in κ_s across the tropopause, reflecting the corresponding discontinuity in N . The κ_s field has been smoothed by retaining only its zonal harmonic components of $k=0\sim 4$, so as to be consistent with defining a waveguide structure for free stationary Rossby waves in the stratosphere.

It should be noted that the wave-activity flux and refractive index used in this study have been derived under WKB-type approximations of the sufficient slowness of zonal and time variations in a basic flow. Unlike in the troposphere, the validity of the approximations is not immediately obvious in the stratosphere, where only a few lowest zonal harmonics of planetary waves are allowed to propagate. As discussed in NH02 and NN04, the validity of the assumptions in our application may be justified *only a posteriori in a qualitative sense* by assessing a degree of localization of the wave-activity flux and its geographical

correspondence with localized waveguide structure as revealed by the refractive index. Therefore, our argument in the rest of the study must be kept qualitative.

3. A LARGE-SCALE CYCLOGENETIC EVENT IN AUGUST 1997

(a) *Mechanisms of the cyclogenesis*

As a typical example of a lower-stratospheric Rossby wave train influencing the tropospheric circulation, an event of large-scale cyclogenesis that occurred around 10 August of 1997 off the Antarctic coast to the south of Australia is investigated in this section. The quasi-stationary nature of the cyclogenesis is apparent in unfiltered sea-level pressure maps shown in Figs. 3a-c. Over the 5-day period centred at 10 August, the cyclone centre exhibited its eastward phase migration of only ~ 2000 km, which is substantially slower than a typical migration speed of an extratropical cyclone. In the reanalysis data, the surface cyclone centre deepened below 960 hPa on that day. The surface cyclogenesis was associated with the intensification of upper-tropospheric cyclonic anomalies (denoted by a square in Figs. 3d-f) within the subpolar jet (SPJ § ; see also Fig. 6a). The centres of the surface cyclone and the cyclonic anomalies aloft (the former is also denoted by a square in Figs. 3a-c) almost coincided with one another, indicative of their nearly equivalent barotropic structure typical for low-frequency tropospheric anomalies over the ocean (Blackmon *et al.* 1979). An incoming wave-activity flux into the cyclonic anomalies from the tropospheric anticyclonic anomalies upstream was modest (Figs. 3d-f), and the barotropic feedback forcing from migratory synoptic-scale transient eddies, as evaluated in a

§ It is also referred to as a polar-front jet.

manner described in Nakamura *et al.* (1997), on the cyclonic anomalies was quite weak (not shown).

In the lower stratosphere (50 hPa), strong quasi-stationary anticyclonic anomalies were observed over the Indian Ocean during the same period (Figs. 3g-i). They were located slightly upstream of the developing tropospheric cyclonic anomalies of interest. This vertical structure is well depicted in zonal-height sections along 60°S in Figs. 3j-l ¶. In the lower stratosphere (between the 200 and 50-hPa levels), phase lines of the streamfunction anomalies exhibited an apparent *eastward* tilt with height between the stratospheric anticyclonic anomalies upstream (around 100°E) and the tropospheric cyclonic anomalies downstream (around 130°E, indicated with a square in Figs. 3j-l), suggestive of downward propagation of quasi-stationary Rossby wave activity. Our wave-activity flux diagnosis reveals that the downward injection of wave activity across the tropopause was indeed pronounced within the upstream half of the tropospheric cyclonic anomalies of interest ||. Especially on 8 August (Fig. 3j), when the cyclonic anomalies began to develop, the flux was dominantly downward below and slightly downstream of the stratospheric anticyclonic anomalies, extending vertically into the mid- and lower troposphere. On 10 August (Fig. 3k), the flux was still dominantly downward except in the lower troposphere.

¶ In all the vertical sections in Figs. 3, 5, 9, 12, the wave-activity flux is weighted by pressure as in (1).

Note that the flux was not pressure-weighted but normalized by pressure in NN04.

|| Those anomalies were slowly moving eastward. Strictly speaking, the wave-activity flux plotted in those figures thus represents group-velocity propagation relative to the slowly-moving wave phase (TN01). Since the group velocities of those wave packets are much larger than their phase velocities, the flux depicts the essential features of the observed wave packet propagation (Figs. 3d-j).

For an assessment of the importance of the downward injection of wave activity relative to its horizontal injection in that cyclogenesis, the vertical and horizontal convergence of the wave-activity flux was evaluated separately (Figs. 4a and b, respectively). The vertical and horizontal convergence was found comparable in magnitude around the cyclonic anomalies of interest near the tropopause. Therefore, both contributed to an increase in wave-activity pseudomomentum M^{**} associated with the amplification of the cyclonic anomalies, but the vertical convergence appears to correspond to the increase in M slightly better than the horizontal convergence. Figure 4 thus suggests that the downward wave-activity injection from the lower-stratospheric anomalies was, *at least*, as important as the horizontal injection from the upstream tropospheric anomalies in the particular large-scale cyclogenesis.

It should be noted that, on 12 August (Fig. 3l), the upward wave-activity flux was dominant in the mid- and lower troposphere in and around the cyclonic anomalies of interest, while the flux was still downward across the tropopause converging into them. In the lower troposphere, the upward flux was hinted as early as 10 August (Fig. 3k). The upward flux is consistent with a slight westward phase tilt with height found in the lower-tropospheric portion of the cyclonic anomalies (Figs. 3k-l), indicative of a contribution from baroclinic processes to the amplification of the cyclonic anomalies. In fact, the anomalies developed above an intense oceanic frontal zone (the Antarctic Polar Frontal Zone) along the Antarctic Circumpolar Current that accompanies sharp surface temperature gradient (Nakamura and Shinpo 2004). It is thus conjectured that

** A quantity M , which is independent of wave phase, is a linear combination of two quantities, one is proportional to wave enstrophy and the other to wave energy (TN01). Convergence (divergence) of the wave-activity flux acts to increase (decrease) M locally.

the upper-tropospheric cyclonic anomalies whose development had been initiated by the downward wave-activity injection from the lower stratosphere (Fig. 3d) induced the thermal advection across the near-surface baroclinic zone, rendering the anomalies slightly baroclinic (c.f. Nakamura and Fukamachi 2004). This baroclinic structure must be favorable for the further amplification of the anomalies within the tropospheric subpolar jet. Nevertheless, Figs. 3 and 4 suggest that the downward propagation of the Rossby wave train from the stratosphere contributed substantially to the initial development of the cyclonic anomalies of interest.

(b) *Evolution of a lower-stratospheric wave train*

A few days before the tropospheric cyclogenesis of interest, the aforementioned anticyclonic anomalies developed at the 50-hPa level over the South Indian Ocean, downstream of the accompanying cyclonic anomalies over the South Atlantic (Fig. 5b). At that level, the horizontal wave-activity flux was predominantly eastward across those two anomaly centres both located at $\sim 60^\circ\text{S}$. It is thus suggested that these anticyclonic and cyclonic anomalies were associated with a quasi-stationary Rossby wave train propagating along the lower-stratospheric PNJ. The flux was strongly divergent in the upstream portion of the cyclonic anomalies, where the flux was predominantly upward across the 150-hPa level. By August 4 (Fig. 5b), another cyclonic anomalies developed over the South Pacific with a wave-activity flux diverging downstream. Again, the wave-activity flux was strongly upward across the 150-hPa level in the upstream portion of these cyclonic anomalies.

The vertical structure of the two wave trains on 4 August is elucidated in a zonal-height section in Fig. 5c. The lower-stratospheric anticyclonic anomalies

over the South Indian Ocean, from which part of the associated wave activity was injected downward into the tropospheric cyclonic anomalies under amplification (denoted by a square as in Figs. 3j-l), developed as a component of the lower-stratospheric Rossby wave train that had emanated from a tropospheric anticyclonic ridge located as far upstream as around the Drake Passage ($90^\circ \sim 60^\circ\text{W}$, denoted by a circle in Fig. 5c). Associated streamfunction anomalies exhibited an apparent westward tilt of phase lines with height, which is consistent with the upward emanating wave-activity flux associated with the wave train. The other wave train was found to emanate from another anticyclonic ridge located southwest of New Zealand (indicated with a triangle in Figs. 3j and 5c). Again, the wave train exhibited an obvious westward phase tilt. The latter wave train appears to reinforce the former. Barotropic feedback forcing from migratory eddies contributed positively to the amplification of each of those blocking ridges (not shown). Wave activity that had emanated eastward from the blocking near New Zealand and then propagated along the SPJ across the South Pacific acted to reinforce the blocking ridge around the Drake Passage (Figs. 3d, 5a and 6a).

(c) *Waveguide structure*

It is evident in Figs. 3g-i that the eastward wave-activity propagation at the 50-hPa level tended to be confined to a latitudinal band between 50°S and 60°S , which corresponds to the prominent PNJ at that level (Fig. 6c). The upward wave-activity injection into the stratosphere also tended to be confined to the same latitudinal band along the bottom of the stratospheric PNJ (Fig. 5b). Both at the 50- and 150-hPa levels, the refractive index (κ_s), defined locally for stationary Rossby waves, exhibits a zonally-elongated band of local maxima extending along the PNJ axis from around the Drake Passage to the region

south of New Zealand across the South Atlantic and Indian Ocean (Fig. 7). This waveguide is also evident in a zonal-height section of κ_s along 60°S (Fig. 8b). Around the tropopause level, the waveguide structure appears to be somewhat distorted within a longitudinal sector of κ_s minima over the South Atlantic between 20°W and 40°E, in association with the equatorward displacement of the tropospheric SPJ relative to the PNJ axis (Fig. 6a). This sector is located just downstream of the tropospheric blocking ridge of interest (indicated by a circle in Figs. 6-8). In the lower stratosphere, the waveguide with relatively large κ_s extended zonally along the PNJ above those κ_s minima. The anticyclonic ridge of interest developed at the exit of the Pacific SPJ (denoted as a circle in Figs. 6-8), located right below the entrance of the stratospheric PNJ (Figs. 6, 7 and 8a). It is conjectured that, in the presence of this particular waveguide structure, wave activity that had emanated from the anticyclonic ridge propagated selectively upward into the stratosphere (Fig. 5c), leading to the formation of the wave train along the PNJ. The rest of the wave activity emanated from the ridge was dispersed mainly equatorward over the South Atlantic (Figs. 3d-f).

The downward wave-activity propagation across the tropopause occurred into the developing cyclone of interest, as the leading edge of the wave train approached the PNJ exit around 120°E (Figs. 3j-l). Below that exit, κ_s was particularly large toward the tropospheric SPJ (Fig. 8b). This region acted as a localized vertical waveguide or a “chimney” through which the wave activity could be injected downward into (or could have emanated upward from) the tropospheric cyclonic anomalies. The well-defined entrance and exit of the PNJ as evident in Fig. 6c were apparently a manifestation of the $k=1$ component of the persistent lower-stratospheric planetary waves.

4. A BLOCKING EVENT IN SEPTEMBER 1997

As our another example of downward wave-activity injection across the tropopause, we briefly refer to a blocking event that occurred south of New Zealand in late September of 1997 (denoted by a square in Figs. 9d-f). As evident in Fig. 9f, the blocking anticyclonic anomalies were shallow, confined mostly to the troposphere. Cyclonic anomalies located upstream, in contrast, were deep, extending into the stratosphere. Rossby wave activity was injected into the developing ridge horizontally in the upper troposphere from another anticyclonic anomalies farther upstream over the South Indian Ocean through the tropospheric cyclonic anomalies (Fig. 9d). At the same time, part of wave activity propagating eastward along the lower-stratospheric PNJ was injected downward across the tropopause into the blocking ridge developing to the south of New Zealand (Figs. 9e-f). Consistently, phase lines of the streamfunction anomalies associated with the ridge exhibited a distinct eastward tilt with height (Fig. 9f).

As indicated in Fig. 9f, the quasi-stationary Rossby wave train with deep structure observed on 24 September originated from another tropospheric cyclonic anomalies located farther upstream over the South Atlantic (denoted by a circle in Fig. 9). The cyclonic anomalies remained rather shallow, confined mostly to the troposphere for the past several days. On 20 September (Fig. 9c), the cyclonic anomalies were situated below the anticyclonic anomalies in the stratosphere over the South Atlantic ($60^{\circ}\text{W}\sim 0^{\circ}$). While weak downward injection of wave activity occurred across the tropopause into the upstream portion of the cyclonic anomalies (Figs. 9a-c), wave activity emanated more strongly upward into the stratospheric anomalies from the downstream portion of the tropospheric anomalies (Figs. 9a-f). This upward wave-activity injection occurred where the

stratospheric PNJ partially overlapped with the tropospheric SPJ (Figs. 9g-h). It should be noted that distinct downward injection of wave activity into the blocking ridge of our primary interest did not occur until the leading edge of the stratospheric wave train reached a “chimney” (vertical waveguide) in the exit region of the PNJ to the south of Australia, which was overlapped with the tropospheric SPJ. The “chimney” was marked with local maxima of κ_s (≥ 3.5) extending from the 70-hPa level downward below the tropopause (Fig. 9i).

5. STRATOSPHERIC WAVE TRAINS IN LATE WINTER OF 1997

In the preceding sections two examples were presented in which downward wave-activity injection from lower-stratospheric Rossby wave trains appeared to contribute toward the amplification of large-scale quasi-stationary anomalies in the SH troposphere. In those examples, the stratospheric wave trains propagating along the PNJ had originated from another tropospheric anomalies located far upstream. In this section, we show that such upward and downward injection of quasi-stationary Rossby wave activity across the tropopause was observed over the SH rather frequently during late winter and early spring of 1997.

Figure 10 shows zonal-time sections of low-pass-filtered geopotential height anomalies at the (a) 50-hPa and (b) 400-hPa levels averaged between 50°S and 60°S. This latitudinal band approximately corresponds to the stratospheric PNJ. This figure is almost the same as Fig. 12a of NN04, but downward wave-activity propagation across the 150-hPa level is now indicated explicitly. As discussed in NN04, formation of a zonally propagating quasi-stationary wave train occurred frequently in the lower stratosphere in conjunction with enhanced upward wave-activity injection across the 150-hPa level (Fig. 10a). One may notice that the

event of the lower-stratospheric wave train examined in our first example was one of the earliest among such events as observed in the particular season. Though less frequently than the upward propagation, the downward wave-activity injection across the 150-hPa level did occur occasionally just downstream of an eastward propagating wave train at the 50-hPa level. The downward wave-activity injection tended to be observed right over or slightly upstream of quasi-stationary 400-hPa height anomalies from which the wave-activity flux diverged eastward (Fig. 10b). In many of those occasions including the two examples shown in the preceding sections, Rossby wave trains that had originated from the tropospheric circulation anomalies propagated zonally in the lower stratosphere, and they were then refracted back into the troposphere to form another wavetrains downstream.

Figure 11 also summarizes the activity of quasi-stationary submonthly fluctuations in the lower stratosphere and upper troposphere, an associated three-dimensional flux of stationary Rossby waves and the time-mean structure of the westerly jets for the three 31-day periods of 17 July-16 August, 17 August-16 September and 16 September-16 October. This figure corresponds to Figs. 9-11 in NN04, but unlike in those figures, regions of downward wave-activity propagation are explicitly indicated. As pointed out by NN04 and confirmed by comparing the left and right columns of Fig. 11, the upward wave-activity propagation tended to be pronounced in regions below the lower-stratospheric PNJ where the tropospheric submonthly fluctuations were particularly strong. In good agreement with Fig. 10, downward wave-activity injection into the troposphere was pronounced right below or slightly downstream of local maxima of 50-hPa submonthly height fluctuations (Figs. 11a, d and g), located right over or slightly upstream of the local maxima of the tropospheric submonthly fluctuations (Figs. 11c, f and i).

This result is suggestive of the significant influence of stratospheric Rossby-wave anomalies that can be exerted on the development of tropospheric quasi-stationary anomalies. As consistent with Fig. 10, the downward wave-activity injection occurred mainly to the south of Australia and in the central South Pacific (Figs. 11c and f), both along the tropospheric SPJ (Fig. 11b and e). After mid-September (Fig. 11i), the downward injection weakened in the central South Pacific, while it was enhanced around the Drake Passage, which is also along the SPJ, located just downstream of the exit of the secondary PNJ core that formed over the eastern South Pacific (Fig. 11h). Still, the region south of Australia remained as the primary region of the downward wave-activity injection. In this region, the downward injection from the stratosphere was so dominant that the wave-activity flux across the 150-hPa level was pointing *downward* even as the *net* over each of the 31-day periods (Fig. 11a, d and g). In the two other regions, the upward wave-activity propagation into the stratosphere dominated over the downward injection, which rendered the net wave-activity flux at the 150-hPa level weakly upward in all of the three periods (Figs. 11a, d and g). In each of those regions of active downward wave-activity injection, a local “chimney” structure with vertically extending κ_s maxima is apparent in association with the overlapping of the stratospheric PNJ and tropospheric SPJ (Fig. 12).

6. CONCLUDING REMARKS

In our case study of the SH circulation in 1997, we have presented several pieces of evidence that wave activity associated with a zonally propagating quasi-stationary Rossby wave train along the lower-stratospheric PNJ that has emanated from quasi-stationary tropospheric anomalies developing at a particular

location can, in some occasions, be injected downward into the troposphere, contributing to the development of another tropospheric anomalies at a distant location, as illustrated schematically in Fig. 2. In one of our examples, the downward propagation of Rossby wave activity across the tropopause contributed to large-scale quasi-stationary cyclogenesis to the south of Australia. In our another example, such downward wave-activity propagation contributed to the formation of a blocking ridge in nearly the same region.

For a quasi-stationary Rossby wave packet that consists mainly of the $k=1, 2$ and 3 components, the stratospheric PNJ with a large wind speed and tight PV gradient acts as a better waveguide than the tropospheric SPJ does. Therefore, Rossby wave activity, once injected into the lower-stratospheric PNJ, propagates eastward through the PNJ nearly twice as fast as it would through the SPJ, thus effectively transferring wave activity downstream. During the August event, we found that the $k=3$ component, which constituted the zonally-confined, “beam-like” wave packet in the lower stratosphere, accounted for nearly 20% of the amplitude of the whole streamfunction anomalies along the PNJ at the 50-hPa level.

At this stage, we are not quite certain whether wave-activity injection across the tropopause alone could trigger the development of the tropospheric anomalies of interest in our examples. Circulation anomalies initiated in the SPJ by tropospheric processes would amplify through downward injection of Rossby wave activity across the tropopause if another anomalies with the opposite sign are or have already been present slightly upstream in the exit of the lower-stratospheric PNJ. It should be stressed that, as mentioned in section 2, our argument must remain qualitative because of the WKB-type assumptions implicit

in our particular diagnosis tools whose validity is not immediately obvious in the stratosphere. Nevertheless, our examples, especially the first one, suggest a potential importance of the downward propagation of a Rossby wave train from the stratosphere at the early stage of the development of large-scale tropospheric anomalies.

An implication of our case study is that realistic representation of the three-dimensional waveguide structure associated with the lower-stratospheric PNJ, including those “chimneys”, in an operational model is potentially an important factor for successful extended weather forecasts in the cold season. Another implication of our study is that in the study of quasi-stationary tropospheric circulation anomalies in the wintertime extratropics, wave-activity injection from lower-stratospheric wave trains must be considered as a possible contributor to their development.

As mentioned in the introduction, the dynamical linkage between the stratosphere and troposphere has been discussed primarily in the context of SSW and/or the annular modes, in relation to the interaction between the entire polar vortex and planetary waves. Among those literature, one may think PH03, in which downward wave propagation from the stratosphere to the troposphere is discussed, may be similar to our analysis. As already mentioned, however, the mechanisms discussed in PH03 differ fundamentally from those in our examples. PH03 discussed the critical layer reflection of the entire planetary waves embedded in the zonally uniform westerlies, which should be distinguished from the downward wave-activity injection in our examples due to the *refraction* of a zonally-confined Rossby wave packet in the vertically sheared westerlies through their “prism” effect (Fig. 1). Thus, downward influence on the tropospheric

circulation tends to be more localized in our examples than the correspondent influence in PH03 or associated with the annular modes.

It has been shown in our study that zonal asymmetries in the time-mean westerlies are important, even over the SH, for zonal and vertical propagation of Rossby wave trains. Specifically, the vertical overlapping of the stratospheric PNJ with the tropospheric SPJ is of particular importance in the local formation of a vertical waveguide across the tropopause through which a quasi-stationary Rossby wave train can propagate upward or downward. If such a cross-tropopause “chimney” forms around the exit region of the lower-stratospheric PNJ, downward wave-activity injection is possible through which a stratospheric Rossby wave train can contribute to the large-scale cyclogenesis or blocking formation in the troposphere. This is likely the reason why downward wave-activity injection into the troposphere during late winter of 1997 occurred most frequently to the south of Australia, where the overlapping of the PNJ exit and the SPJ was observed throughout the season. The location of such a “chimney” must be sensible to the three-dimensional structure of planetary waves included in the time-mean flow. We thus conjecture that the seasonal and interannual changes in positions of the PNJ exits could result in the modulation of the downward propagation of quasi-stationary Rossby wave activity into the troposphere in the two hemispheres, which will be a topic for our future study.

ACKNOWLEDGEMENTS

The authors are grateful to Dr. I. Hirota for careful reading of the earlier version of manuscript and giving us valuable comments and advice. They are also grateful to Drs. T. J. Dunkerton, D. J. Karoly and B. J. Hoskins for their

useful comments and encouragement. Comments by the two anonymous referees and the editor (Dr. M. Jackes) are greatly acknowledged. This study is supported by the JSPS-KAKENHI (B) 15340153. The Grid Analysis and Display System (GrADS) was used for drawing most of the figures.

REFERENCES

- Baldwin, M. P. and Dunkerton, T. J. 1999 Propagation of the Arctic Oscillation from the stratosphere to the troposphere. *J. Geophys. Res.*, **104**, 30937–30946
- Boville, B. A. 1984 The influence of the polar night jet on the tropospheric circulation in a GCM. *J. Atmos. Sci.*, **41**, 1132–1142
- Blackmon, M. L., Madden, R. A., Wallace, J. M. and Gutzler, D. S. 1979 Geographical variations in the vertical structure of geopotential height fluctuations. *J. Atmos. Sci.*, **36**, 2450–2466
- Chen, P. and Robinson, W. A. 1992 Propagation of planetary waves between the troposphere and stratosphere. *J. Atmos. Sci.*, **49**, 2533–2545
- Christiansen, B. 2001 Downward propagation of zonal mean zonal wind anomalies from the stratosphere to the troposphere: Model and reanalysis. *J. Geophys. Res.*, **106**, 27307–27322
- Geller, M. A. and Alpert, L. C. 1980 Planetary wave coupling between the troposphere and the middle atmosphere as a possible sun-weather mechanism. *J. Atmos. Sci.*, **37**, 1197–1215
- Harnik, N. 2002 The evolution of a stratospheric wave packet. *J. Atmos. Sci.*, **59**, 202–217
- Hartley, D. E., Villarin, J. T., Black, R. X. and Davis, C. A. 1996 A new perspective on the dynamical link between the stratosphere and troposphere. *Nature*, **391**, 471–473
- Hirota, I. and Sato, Y. 1969 Periodic variation of the winter stratospheric circulation and intermittent vertical propagation of planetary waves. *J. Meteorol. Soc. Jpn.*, **47**, 390–402
- Hoskins, B. J. and Ambrizzi, T. 1993 Rossby wave propagation on a realistic longitudinally varying flow. *J. Atmos. Sci.*, **50**, 1661–1671
- Karoly, D. J. and Hoskins, B. J. 1982 Three dimensional propagation of planetary waves. *J. Meteorol. Soc. Jpn.*, **60**, 109–123
- Karoly, D. J. 1983 Rossby wave propagation in a barotropic atmosphere. *Dyn. Atmos. Oceans*, **7**, 111–125
- Kodera, K., Yamazaki, K., Chiba, M. and Shibata, K. 1990 Downward propagation of upper stratospheric mean zonal wind perturbation to the troposphere. *Geophys. Res. Lett.*, **17**, 1263–1266
- Kodera, K., Chiba, M. and Shibata, K. 1991 A possible influence of the polar night stratospheric jet on the subtropical tropospheric jet. *J. Meteorol. Soc. Jpn.*, **69**, 715–745

- Kodera, K. and Chiba, M. 1995 Tropospheric circulation changes associated with stratospheric sudden warmings: A case study. *J. Geophys. Res.*, **100**, 11055–11068
- Kodera, K., Kuroda Y. and Pawson, S. 2000 Stratospheric sudden warmings and slowly propagating zonal-mean zonal wind anomalies. *J. Geophys. Res.*, **105**, 12351–12359
- Kodera, K. and Kuroda, Y. 2000a A mechanistic model study of slowly propagating coupled stratosphere-troposphere variability. *J. Geophys. Res.*, **105**, 12361–12370
- 2000b Tropospheric and stratospheric aspects of the Arctic Oscillation. *Geophys. Res. Lett.*, **27**, 3349–3352
- Kuroda, Y. and Kodera, K. 1999 Role of planetary waves in the stratosphere-troposphere coupled variability in the Northern Hemisphere winter. *Geophys. Res. Lett.*, **26**, 2375–2378
- 2001 Variability of the polar night jet in the Northern and Southern Hemispheres. *J. Geophys. Res.*, **106**, 20703–20713
- Kalnary, M. E., Kanamitsu, M., Kistler, R., Collins, W., Deaven, D., Gandin, L., Iredell, M., Saha, S., White, G., Woollen, J., Zhu, Y., Leetmaa, A., Reynolds, R., Chelliah, M., Ebisuzaki, W., Higgins, W., Janowiak, J., Mo, K. C., Ropelewski, W., Wang, J., Jenne, R. and Joseph, D. 1996 The NCEP/NCAR 40-year reanalysis project. *Bull. Am. Meteorol. Soc.*, **77**, 437–471
- Matsuno, T. 1971 A dynamical model of the stratospheric sudden warming. *J. Atmos. Sci.*, **28**, 1479–1494
- Nakamura, H., Nakamura, M. and Anderson, J. L. 1997 The role of high- and low-frequency dynamics in blocking formation. *Mon. Weather Rev.*, **125**, 2074–2093
- Nakamura, H. and Honda, M. 2002 Interannual seesaw between the Aleutian and Icelandic lows Part III: Its influence upon the stratospheric variability. *J. Meteorol. Soc. Jpn.*, **80**, 1051–1067
- Nakamura, H. and Fukamachi, T. 2004 Evolution and dynamics of summertime blocking over the Far East and the associated surface Okhotsk high. *Q. J. R. Meteorol. Soc.*, **130**, 1213–1233
- Nakamura, H. and Shimpo, A. 2004 Seasonal variations in the Southern Hemisphere storm tracks and jet streams as revealed in a reanalysis data set. *J. Climate*, **17**, 1828–1844
- Nishii, K. and Nakamura, H. 2004a Rossby wave trains in the lower stratosphere of the Southern Hemisphere: A case study for late winter of 1997. *Q. J. R. Meteorol. Soc.*, **130**, 325–346
- 2004b Tropospheric influence on the diminished Antarctic ozone hole in September 2002. *Geophys. Res. Lett.*, **31**, –, doi:10.1029/GL019532, *in press*
- Plumb, R. A. 1985 On the three-dimensional propagation of stationary waves. *J. Atmos. Sci.*, **42**, 217–229
- Perlwitz, J. and Harnik, N. 2003 Observational evidence of a stratospheric influence on the troposphere by planetary wave reflection. *J. Climate*, **16**, 3011–3026

- Polvani, L. M. and Kushner, P. J. 2002 Tropospheric response to stratospheric perturbations in a relatively simple general circulation model. *Geophys. Res. Lett.*, **29**, 1114–,doi:10.1029/2001GL014284
- Randel, W. J. 1988 The seasonal evolution of planetary waves in the Southern Hemisphere stratosphere and troposphere. *Q. J. R. Meteorol. Soc.*, **114**, 1385–1409
- Shiotani, M. and Hirota, I. 1985 Planetary wave-mean flow interaction in the stratosphere: a comparison between northern and southern hemispheres. *Q. J. R. Meteorol. Soc.*, **111**, 309–334
- Takaya, K. and Nakamura, H. 2001 A formulation of a phase-independent wave-activity flux for stationary and migratory quasi-geostrophic eddies on a zonally basic flow. *J. Atmos. Sci.*, **58**, 608–627
- Thompson, D. W. J. and Wallace, J. M. 2001 Regional climate impacts of the Northern Hemisphere annular mode. *Science*, **293**, 85–89
- Yoden, S., Yamaga, T., Pawson, S. and Langematz, U. 1999 A composite analysis of the stratospheric sudden warmings simulated in a perpetual January integration of the Berlin TSM GCM. *J. Meteorol. Soc. Jpn.*, **77**, 431–445
- Zhou, S. T, Miller, A. J., Wang, J. and Angell, J. K. 2002 Downward-propagating temperature anomalies in the preconditioned polar stratosphere. *J. Climate*, **15**, 781–792

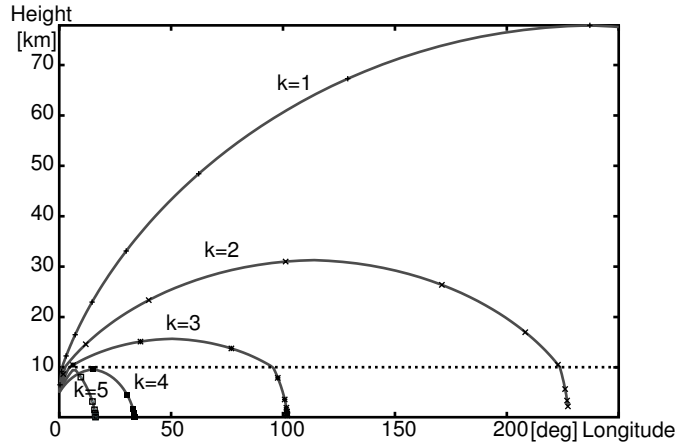


Figure 1. Ray tracing of stationary Rossby waves in a β channel at 60°S for individual zonal harmonics with zonal wavenumbers (k) 1 through 5 as indicated. The background westerlies are zonally homogeneous with a uniform vertical shear of $10 \text{ [m s}^{-1}/10\text{km]}$ and no surface wind. Scale height (H) is fixed to 10 [km] . The “tropopause” is placed at the altitude of $z = H$, and the Brunt-Väisälä frequency is set to $0.02 \text{ [s}^{-1}]$ and $0.01 \text{ [s}^{-1}]$ above and below $z = H$, respectively. Distance between any pairs of symbols along each of the rays corresponds to the distance over which the ray can travel in a particular 24-hour period.

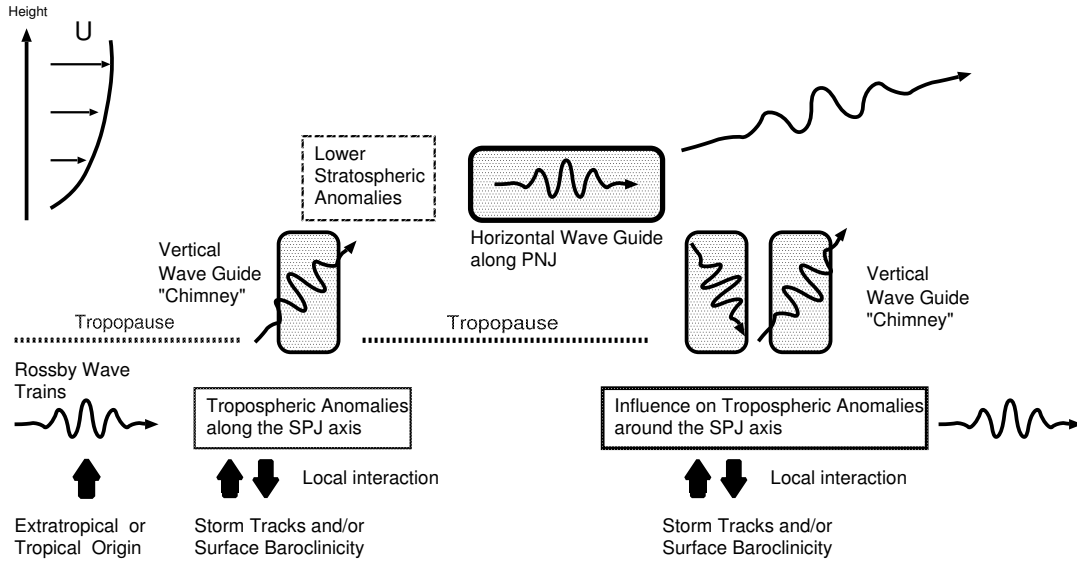


Figure 2. Schematic diagram of a quasi-stationary Rossby wave train with a tropospheric origin propagating in the lower stratosphere. Because of the “prism effect” of the vertically sheared PNJ, only the wave activity associated with the lowest zonal wavenumber(s) can keep propagating farther upward. The rest of the wave activity associated with higher wavenumbers can be refracted back downward to the troposphere if the wave train reaches the PNJ exit where a vertical waveguide (or “chimney”) forms. The downward injected wave activity can trigger the development of tropospheric anomalies locally, which can further amplify in the presence of feedback forcing from a local storm track and/or through interaction with near-surface baroclinicity.

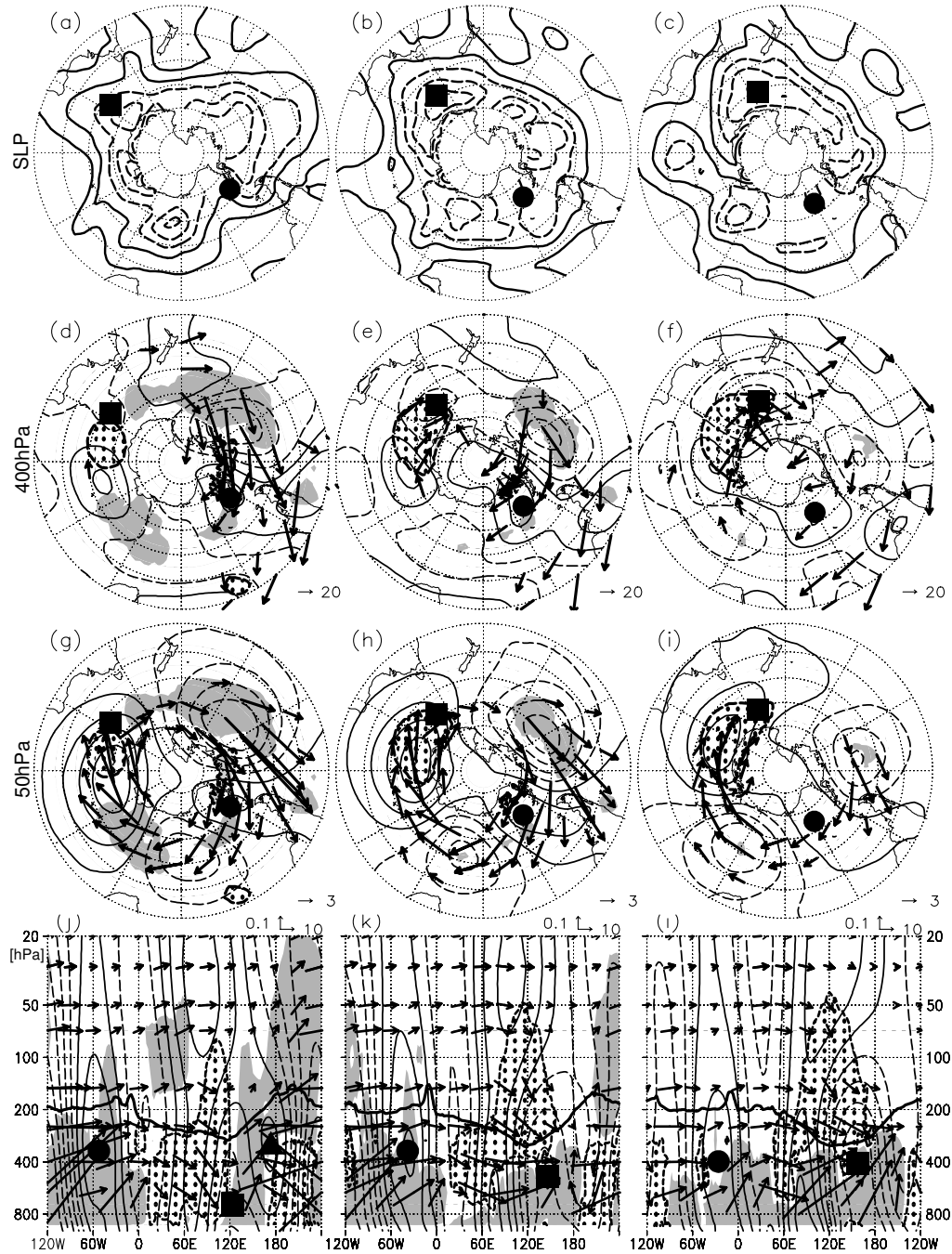


Figure 3. (a-c) Maps of unfiltered sea-level pressure for (a) 8, (b) 10 and (c) 12 August, 1997. Solid lines are for 1005 and 1020 hPa, and dashed lines for 960, 975 and 990 hPa. (d-f) As in (a-c), respectively, but for 8-day low-pass-filtered geopotential height anomalies (contoured for ± 50 , ± 150 and ± 250 m), and the horizontal component of an associated wave-activity flux (arrows) at the 400-hPa level. Solid and dashed lines represent anticyclonic (positive) and cyclonic (negative) anomalies, respectively. Scaling for the arrows is given at the lower-right corner of each panel [Unit: $\text{m}^2 \text{s}^{-2}$]. Shading and stippling indicate the upward and downward components, respectively, of the wave-activity flux at the 150-hPa level whose magnitude exceeds $0.03 [\text{m}^2 \text{s}^{-2}]$. A square indicates the 400-hPa cyclonic anomaly centre associated with the surface cyclone of interest, as also plotted in (a-c). A circle and triangle denote the two 400-hPa anticyclonic anomaly centres referred to in the text (also in other panels). (g-i) As in (d-f), respectively, but for 8-day low-pass-filtered 50-hPa geopotential height anomalies (contoured for ± 60 , ± 180 , ± 300 and ± 420 m), and the horizontal component of an associated wave-activity flux at the 50-hPa level (arrow). (j-l) Zonal sections for 60°S of geopotential height anomalies (contoured for ± 30 , ± 90 , ± 150 and ± 210 m) and an associated wave-activity flux (arrows). Scaling for the arrows is given near the upper-right corner of each panel [Unit: $\text{m}^2 \text{s}^{-2}$]. Shading and stippling indicate the upward and downward components, respectively, of the wave-activity flux whose magnitude exceeds $0.03 [\text{m}^2 \text{s}^{-2}]$. The anomalies have been normalized with pressure. The 5-day mean tropopause defined by the NCEP is indicated with a thick solid line.

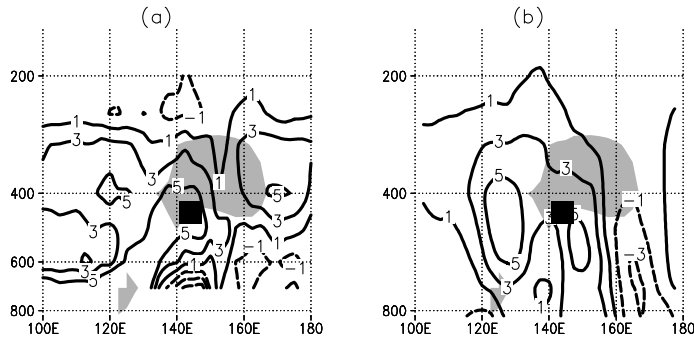


Figure 4. Zonal sections for 60°S over a longitudinal sector $[100^\circ\text{E}\sim 180^\circ]$ of (a) vertical and (b) horizontal convergence of a wave-activity flux (contoured for $-1, 1, 3, 5 \text{ [m s}^{-1}/\text{day]}$), respectively, for 10 August 1997. Shading denotes the time tendency of M defined in TN01 larger than $5 \text{ m s}^{-1}/\text{day}$. The tendency was evaluated from anomaly data by centred differencing. In (a) and (b), solid and dashed lines represent the flux convergence (positive) and divergence (negative), respectively. A square denotes the centre of the cyclonic anomalies of interest.

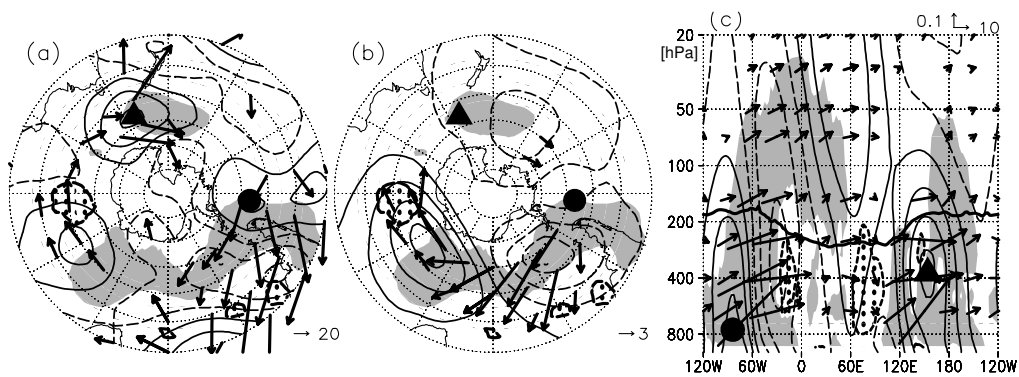


Figure 5. (a-c) As in Figs. 3(d, g, j), respectively, but for 4 August.

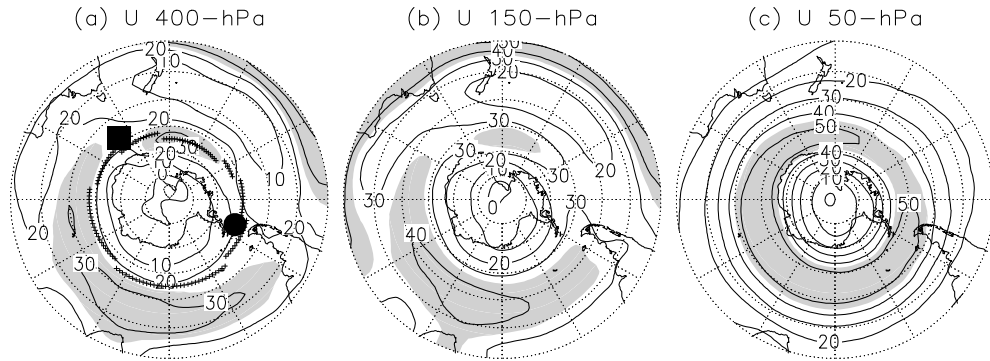


Figure 6. Mean westerly wind speed (U ; contoured for every 10 m s^{-1}) for the 31-day period centred at August 10 at the (a) 400-hPa, (b) 150-hPa and (c) 50-hPa levels. Shading: (a) $U \geq 25 \text{ [m s}^{-1}]$, (b) $U \geq 35 \text{ [m s}^{-1}]$, (c) $U \geq 45 \text{ [m s}^{-1}]$. A line of small crosses in (a) indicates the 50-hPa PNJ axis plotted in (c). A circle and square indicate the same 400-hPa anomaly centres on August 10 as plotted in Fig. 3.

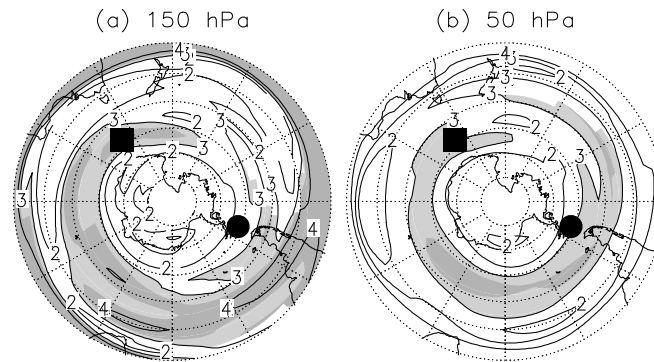


Figure 7. Maps of the refractive index κ_s for stationary Rossby waves represented as the “equivalent zonal wavenumber” for each latitude (i.e. κ_s divided by the earth radius and cosine of each latitude) at the (a) 150-hPa and (b) 50-hPa levels, both based on the mean circulation over the 31-day period centred at 10 August, 1997. Light and heavy shading indicates regions where $\kappa_s \geq 3$ and 3.5 , respectively, and $U \geq 25 \text{ [m s}^{-1}]$. A circle and square indicate the same 400-hPa anomaly centres on August 10 as plotted in Fig. 3.

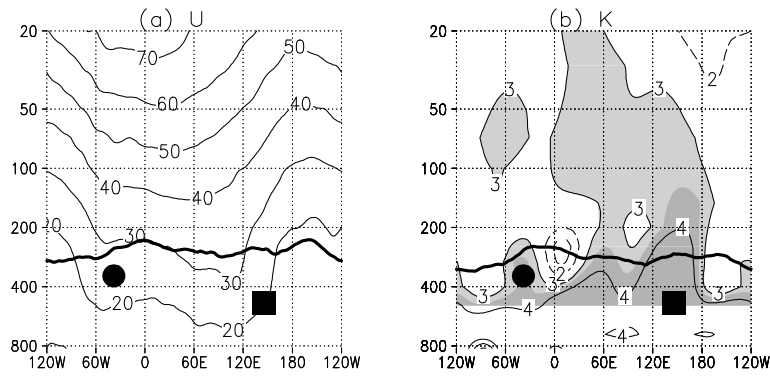


Figure 8. Zonal sections for 60°S of (a) westerly wind speed (U ; every 10 m s^{-1}) and (b) refractive index (κ_s) for stationary Rossby waves, both based on the mean circulation in the 31-day period centred at 10 August, 1997. κ_s is represented as the equivalent zonal wavenumber for this latitude circle. Shading conventions in (b) are the same as in Fig. 7. Heavy lines represent the tropopause. A circle and square indicate the same anomaly centres on August 10 as plotted in Fig. 3.

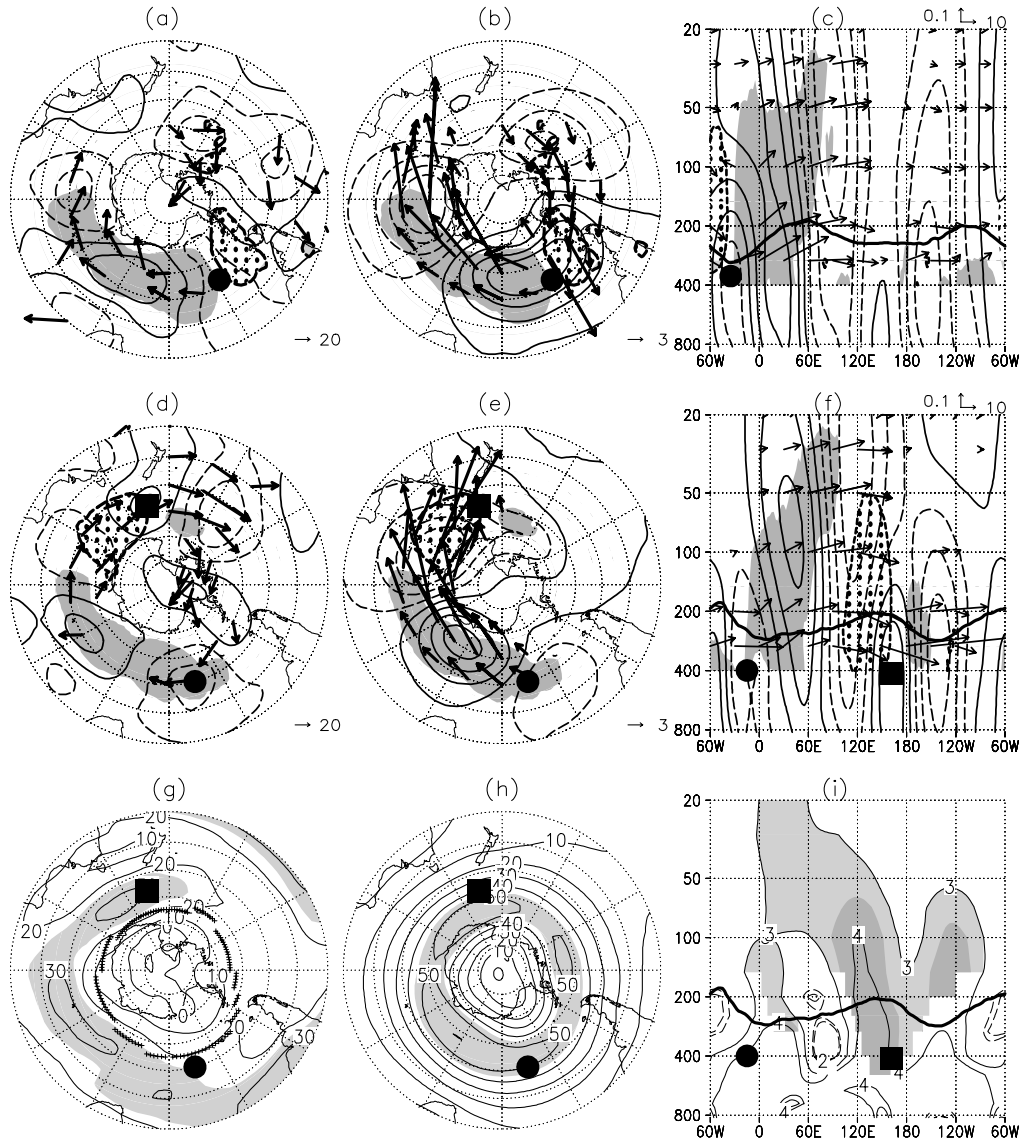


Figure 9. (a-c) Same as in Figs. 3d, g and j, respectively, but for 20 September, 1997. (d-i) Same as in Figs. 3d, 3g and 3j, 6a, 6c and 8b, respectively, but for 24 September 1997.

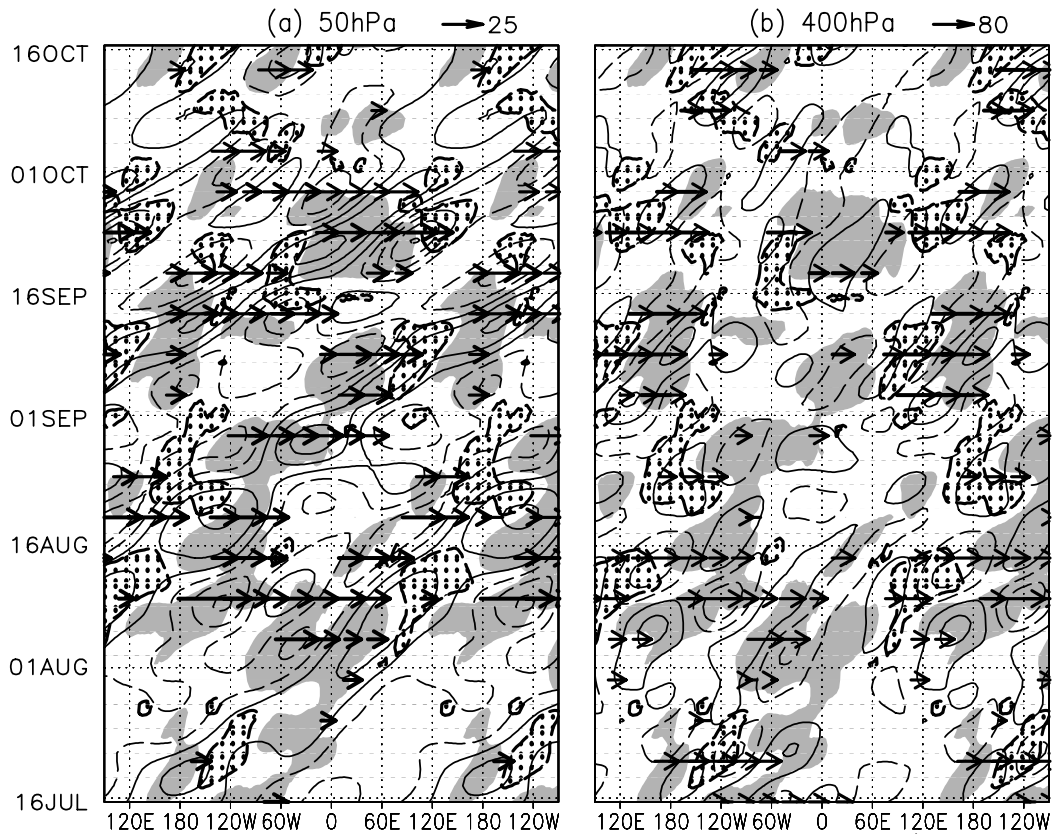


Figure 10. Zonal-time sections for our analysis period (16 July ~ 16 October, 1997) of geopotential height anomalies and the zonal component of a wave-activity flux (arrows), based on the meridional averaging between 55°S and 60°S at the (a) 50-hPa and (b) 400-hPa levels. Solid and dashed lines indicate anticyclonic and cyclonic height anomalies, respectively. Contours are drawn for (a) ± 150 , ± 450 , ± 750 , ± 1050 and ± 1350 m, and for (b) ± 100 , ± 300 and ± 500 m. Scaling for the arrows is given at the upper-right corner of each panel (unit: $\text{m}^2 \text{s}^{-2}$). Shading and stippling indicate the upward and downward components, respectively, of the wave-activity flux across the 150-hPa level whose magnitude exceeds $0.03 [\text{m}^2 \text{s}^{-2}]$.

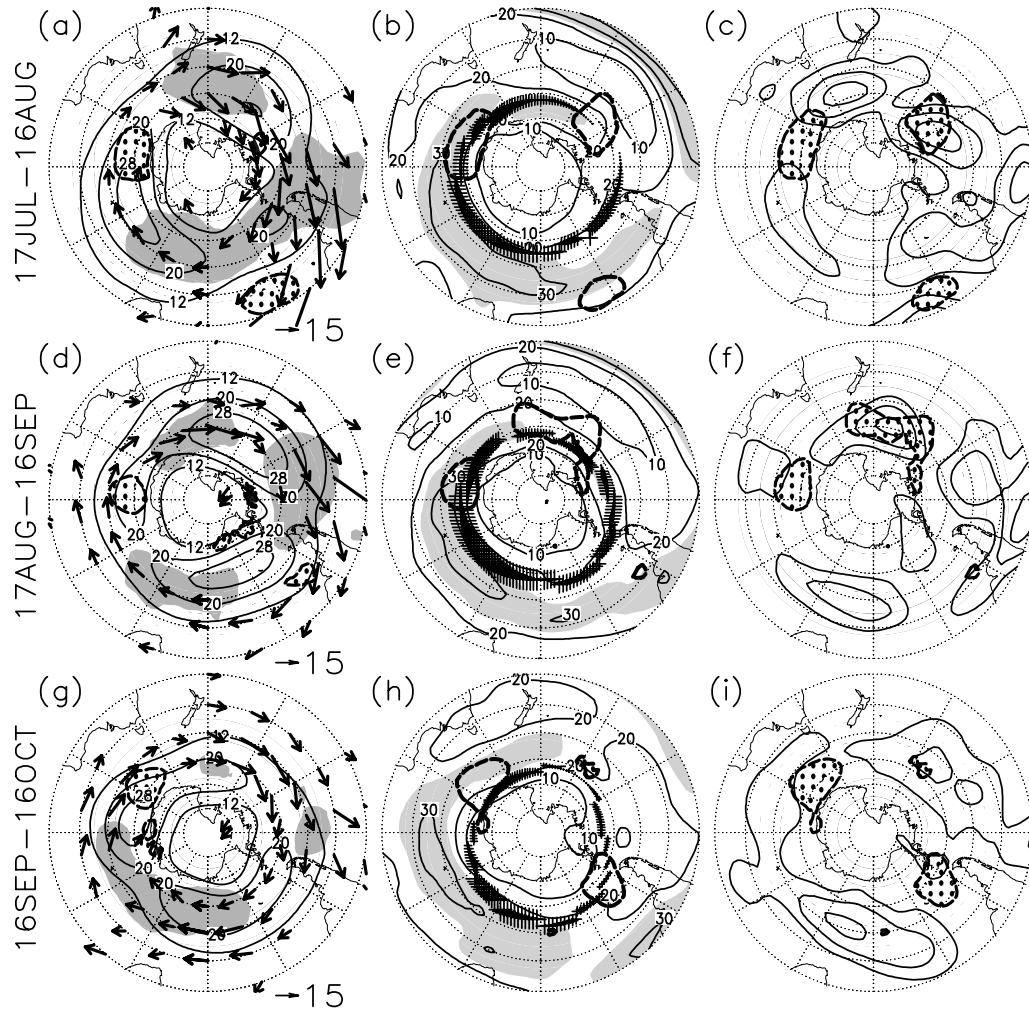


Figure 11. (a) Standard deviation of submonthly low-pass-filtered fluctuations in 50-hPa geopotential height (contoured for 120, 200 and 280 m), and the horizontal component of a time-mean 50-hPa wave-activity flux (arrows). Scaling for the arrows is indicated at the lower-right corner. Shading and stippling are applied to the regions where the vertical component of the 31-day mean *net* wave-activity flux is upward or downward, respectively, at the 150-hPa level, exceeding $0.01 \text{ [m}^2 \text{ s}^{-2}]$ in strength. (b) Mean 400-hPa westerly wind speed (contour interval: 10 m s^{-1}). Small crosses superimposed mark the 50-hPa PNJ axis (their size is proportional to the corresponding local wind speed). Dashed lines surround the regions where the 31-day mean downward wave-activity flux (but not the net flux) at the 150-hPa level was stronger than $0.01 \text{ [m}^2 \text{ s}^{-2}]$ in magnitude. (c) Standard deviation of submonthly low-pass-filtered fluctuations in 400-hPa geopotential height (contoured for 80, 110 and 140 m). Stippling is applied where the 31-day mean downward wave-activity flux as in (b) at the 150-hPa level exceeds $0.01 \text{ [m}^2 \text{ s}^{-2}]$ in magnitude. The periods for (a-c), (d-f) and (g-i) are for 17 July ~ 16 August, 17 August ~ 16 September and 16 September ~ 16 October, respectively.

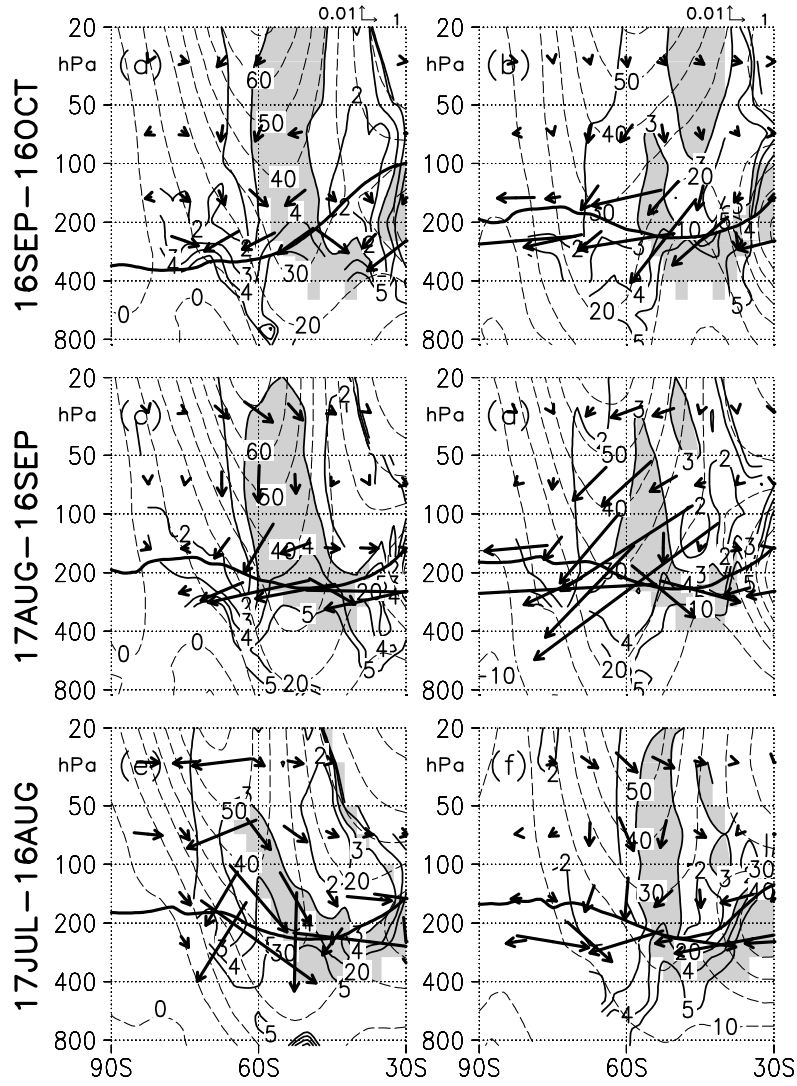


Figure 12. (a) Meridional section of κ_s (solid lines), U (dashed lines for every 10 $[m s^{-1}]$) and the meridional and vertical components of a mean wave-activity flux (arrows), all of which are averaged between $80^\circ E$ and $140^\circ E$ for 17 July ~ 16 August. Shading indicates the regions for $\kappa_s \geq 3$ and $U \geq 25$ $[m s^{-1}]$, and scaling for arrows is given at the right-upper corner of the panel. A thick line indicates the tropopause defined by the NCEP. The wave-activity flux was included in the averaging only when the flux was pointing downward. (b): Same as in (a), but averaged between $110^\circ W$ and $150^\circ W$. (c): Same as in (a), but averaged between $80^\circ E$ and $120^\circ E$ for 17 August ~ 16 September. (d): Same as in (a), but averaged between $160^\circ E$ and $130^\circ W$ for 17 August ~ 16 September. (e): Same as in (a), but averaged between $110^\circ E$ and $150^\circ E$ for 16 September ~ 16 October. (f): Same as in (a), but averaged between $40^\circ W$ and $70^\circ W$ for 16 September ~ 16 October.